



# Statistics of Low Frequency Cutoffs for Type III Radio Bursts Observed by Parker Solar Probe during Its Encounters 1–5

Bing Ma<sup>1,2</sup> , Ling Chen<sup>1,3</sup> , Dejin Wu<sup>1</sup> , and Stuart D. Bale<sup>4,5,6,7</sup>

<sup>1</sup> Key Laboratory of Planetary Sciences, Purple Mountain Observatory, Chinese Academy of Sciences, Nanjing 210023, People's Republic of China  
[clvslc214@pmo.ac.cn](mailto:clvslc214@pmo.ac.cn)

<sup>2</sup> School of Astronomy and Space Science, University of Science and Technology of China, Hefei 230026, People's Republic of China

<sup>3</sup> CAS Key Laboratory of Solar Activity, National Astronomical Observatories, Beijing 100012, People's Republic of China

<sup>4</sup> Space Sciences Laboratory, University of California, Berkeley, CA 94720-7450, USA

<sup>5</sup> Physics Department, University of California, Berkeley, CA 94720-7300, USA

<sup>6</sup> The Blackett Laboratory, Imperial College London, London, SW7 2AZ, UK

<sup>7</sup> School of Physics and Astronomy, Queen Mary University of London, London E1 4NS, UK

Received 2021 February 27; revised 2021 April 16; accepted 2021 April 26; published 2021 May 18

## Abstract

The low frequency cutoffs  $f_{lo}$  and the observed plasma frequency  $f_p$  of 176 type III radio bursts are investigated in this paper. These events are observed by the Parker Solar Probe when it is in the encounter phase from the first to the fifth orbit. The result shows that the distribution of cutoffs  $f_{lo}$  is widely spread between 200 kHz and 1.6 MHz. While the plasma frequency  $f_p$  at the spacecraft is between 50 and 250 kHz, which is almost all smaller than  $f_{lo}$ . The result also shows that the maximum probability distribution of  $f_{lo}$  ( $\sim 680$  kHz) is remarkably higher than that observed by Ulysses and Wind ( $\sim 100$  kHz) in previous research. Three possible reasons, i.e., solar activity intensity, event electing criteria, and radiation attenuation effect, are also preliminarily discussed.

*Unified Astronomy Thesaurus concepts:* [Interplanetary physics \(827\)](#); [Solar radio emission \(1522\)](#)

## 1. Introduction

Type III radio bursts are a typical signature of energetic electron beams ( $v \approx 0.3c$ ) that propagate outward along open magnetic field lines from the corona to interplanetary space (Wild & McCready 1950). There are two important observed characteristics of type III radio bursts. The fast frequency shift from high to low with respect to time is the most critical feature and the other one is the fundamental-harmonic frequency pairs structure in their dynamic spectra (Wild et al. 1954a, 1954b).

One generation mechanism of the type III radio bursts associated with the plasma frequency  $\omega_{pe}$  is called plasma emission, which was proposed by Ginzburg & Zhelezniakov (1958). The main process is that the fundamental (or harmonic) emission is produced by some nonlinear wave-wave coupling between Langmuir waves excited by fast electron beams and ion-acoustic waves (or reverse Langmuir waves). The plasma emission theory is successful in explaining the two important observed features. Whereas it ignores the influence of intense magnetic field in active regions and there are still some disputed problems remaining to get a reasonable explanation (Wu 2012). Considering the effect of magnetic field on the emission generation process, Twiss (1958) and Schneider (1959) presented electron cyclotron maser emission (ECME) as another alternative mechanism at almost the same time as Ginzburg & Zhelezniakov (1958). According to the ECME, the electromagnetic wave could be amplified directly by electron cyclotron maser instability at the electron cyclotron frequency  $\omega_{ce}$  and its harmonic frequencies  $2\omega_{ce}$  (Chen et al. 2017).

Based on the plasma emission mechanism and density model of solar atmosphere, interplanetary (IP) type III bursts (0.01–10 MHz) are deemed to generate in the interplanetary space because their radiation frequencies are lower than solar type III bursts (25–300 MHz) (Lobzin et al. 2014). Wu et al. (2004) found three distinct observed characteristics of IP type III bursts: the sudden termination of emission at low frequencies, very low starting

frequencies, and long duration near the cutoff frequencies. These three features could be well explained by the ECME mechanism combined with the hypothesis of the density-depleted flux tubes model proposed in their papers (Wu et al. 2002, 2004).

For the first feature mentioned above, the low frequency cutoffs of IP type III bursts observed by Ulysses spacecraft have been discussed in detail by Leblanc et al. (1995). Based on the observation by Ulysses from 1990 November to 1994 June at 1.1–4.3 au, they collected in total 1028 type III events to perform the distribution of the cutoff frequency  $f_{lo}$  and the corresponding plasma frequency  $f_p$ . They found that the cutoffs  $f_{lo}$  of type III events is independent of the location of the Ulysses while the distribution of  $f_p$  is consistent with the electron density model of solar wind. They also found that cutoff frequency  $f_{lo}$  mainly ranges from 20 to 300 kHz and is almost all higher than local  $f_p$  at different locations of spacecraft. In addition, the maximum frequency of the distribution of  $f_{lo}$  is approximately 100 kHz. Dulk et al. (1996) utilized the data observed by both Wind and Ulysses spacecraft during the period from 1994 November 18 to 1995 April 16 to explore the low frequency cutoffs at different locations simultaneously. The results show similar conclusions with Leblanc et al. (1995). They suggested that the cutoffs of type III bursts probably are caused by the intrinsic properties of emission mechanism and also affected by the propagation effects such as refraction and scattering.

The previous studies of low frequency cutoffs for type III radio bursts are based on spacecraft at  $\sim 1$  au (Wind) or  $\sim 1.1$ –4.3 au (Ulysses). In this paper, we use the radio data observed by the Parker Solar Probe (PSP) within 0.25 au (during encounter phases) to study the low frequency cutoffs of the type III emission and preliminarily discuss the possible reasons of the different results from previous studies. The rest of the paper is organized as follows. After briefly introducing the PSP spacecraft and relative instruments installed on it, we show our statistical results of low frequency cutoffs  $f_{lo}$  and plasma frequency  $f_p$  for type III radio bursts observed by PSP

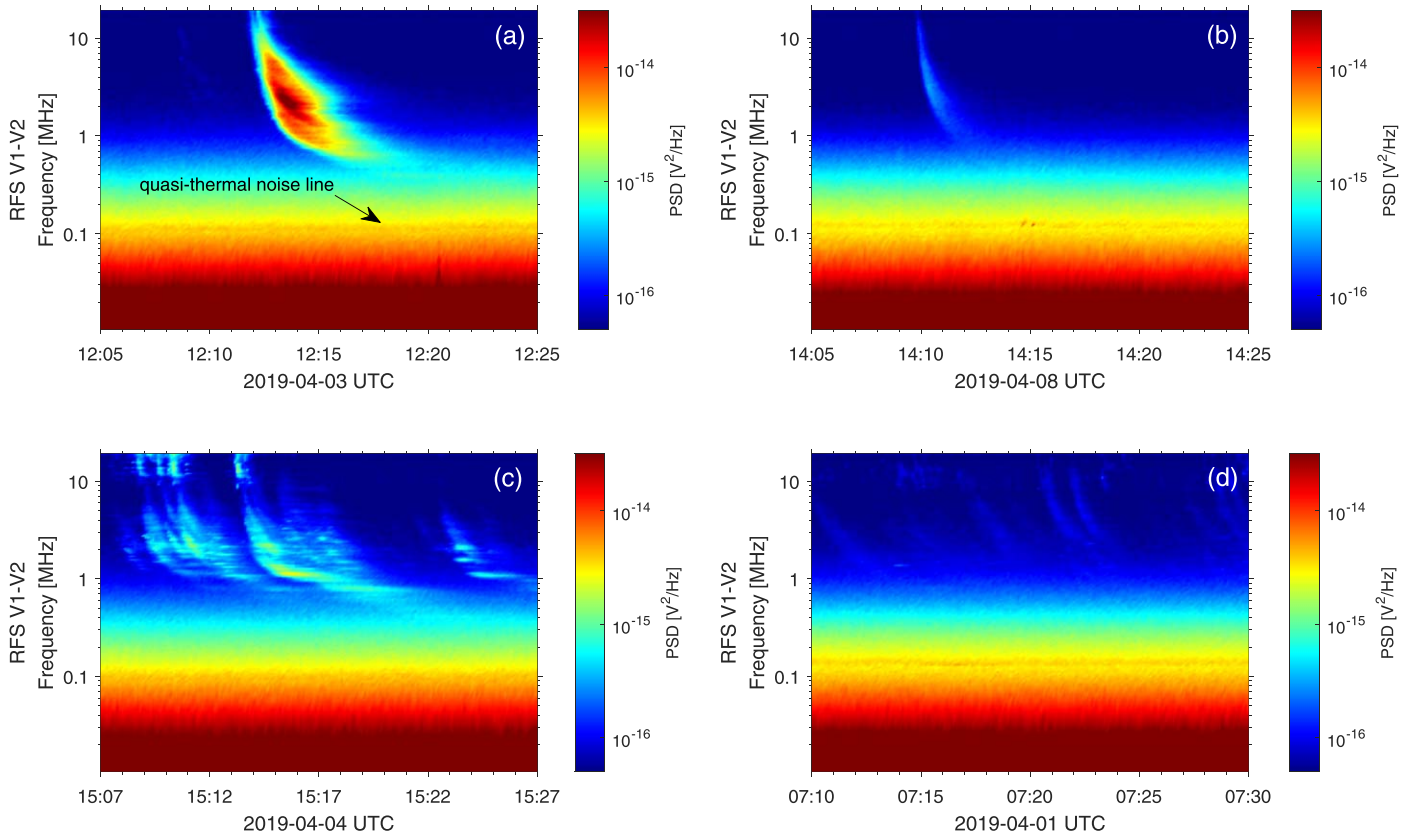


**Figure 1.** Four 20 minute radio dynamic spectra observed by PSP. (a) An intense type III radio burst with a clear low frequency boundary of cutoff. The black arrow indicates the quasi-thermal noise line. (b) Another type III radio burst that can still be identified. (c) Two groups of overlapping bursts for which boundaries cannot be identified clearly because of their overlap. (d) Some relatively weak bursts that cannot be identified.

in Section 2. Finally, in Section 3, we discuss and summarize our findings.

## 2. Observation and Analysis

### 2.1. Spacecraft and Instruments

NASA’s PSP is a spacecraft that was launched on 2018 August 12 and could fly to a closer distance to the Sun than any other previous spacecraft (Fox et al. 2016; Mitchell et al. 2020). The perihelion of PSP’s orbit is getting lower with the assistance of Venus gravity from the initiatory  $35.7 R_{\odot}$  to the closest  $9.86 R_{\odot}$  from the center of the Sun, where  $R_{\odot}$  is the solar radius (Pulupa et al. 2017). Therefore, PSP is the first spacecraft to make the in situ measurements in the solar corona and the source position of the solar wind (Bale et al. 2016). The FIELDS instrument on PSP can provide the measurement of the electric and magnetic field. Four monopole electric field antennas (V1–V4) are installed beside the PSP heat shield, each antenna is 2 meters long (Pulupa et al. 2020). The fifth dipole electric field antenna (V5) is mounted on the magnetometer boom, which is 21 cm long. The radio observation on the FIELDS is finished by the dual-channel receiver named the Radio Frequency Spectrometer (RFS; Pulupa et al. 2017), which covers the bandwidth of 10.5 kHz–19.2 MHz. The Low Frequency Receiver (LFR; 10.5 kHz–1.7 MHz) and the High Frequency Receiver (HFR; 1.3 MHz–19.2 MHz) are the two sub-bandwidths that are used to produce the reduced data products of RFS.

Each orbit of PSP is divided into an encounter phase and a cruise phase. When the distance of PSP from the Sun is within

0.25 au (about  $54 R_{\odot}$ ) the PSP will operate as the encounter mode and all instruments work continuously at a high-rate recording mode. During the encounter phase, RFS records data at a cadence of one spectrum per  $\sim 7$  seconds. On the contrary, when the distance is larger than 0.25 au, all the PSP’s instruments work at the cruise mode and the data-recording cadence of RFS is one spectrum per  $\sim 56$  seconds. In this study, we use the RFS data produced during the encounter phases from the first orbit to the fifth orbit (E01–E05) to obtain the low frequency cutoffs  $f_{lo}$  and plasma frequency  $f_p$  of type III bursts.

### 2.2. Statistical Results and Analysis

According to the data released up to now, we can only obtain the power spectral density (PSD) of radio emission in units of  $V^2 \text{ Hz}^{-1}$  rather than the radio flux density in units of s.f.u. or  $\text{W m}^{-2} \text{ Hz}^{-1}$  depending on the instrument calibrating coefficient. We design a program that takes each 30 minute spectrum as a data block and recognizes individual bursts by judging the intensity of the background-subtracted data. The Channel 0 (V1–V2 auto-spectra) data products of RFS observed during the PSP’s E01 to E05 are recognized by our program automatically. There are in total 247 type III radio events recognized by this program. In order to make the analysis results believable, we check the 247 events manually one by one. At last, only 176 events with a clear boundary of cutoff and a distinct quasi-thermal noise line (Meyer-Vernet 1979) can be selected to get their  $f_{lo}$  and  $f_p$ , respectively. Figures 1(a) and 1(b) display bursts that can be selected by the program. A large number of overlapping type III bursts that cannot be distinguished clearly from each other, as shown in

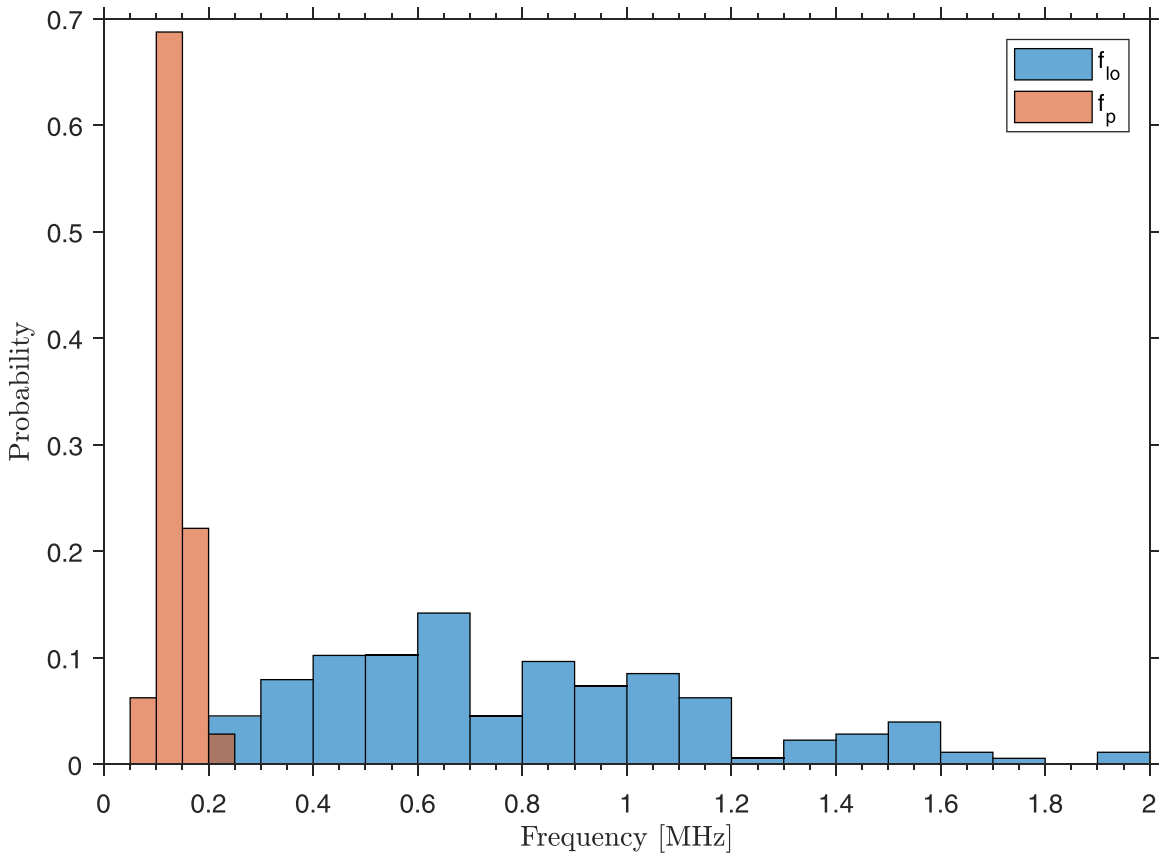


**Figure 2.** The statistical histogram of normalized probability distribution of the cutoff frequency  $f_{lo}$  (the blue bar) and the spacecraft’s in situ plasma frequency  $f_p$  (the orange bar).

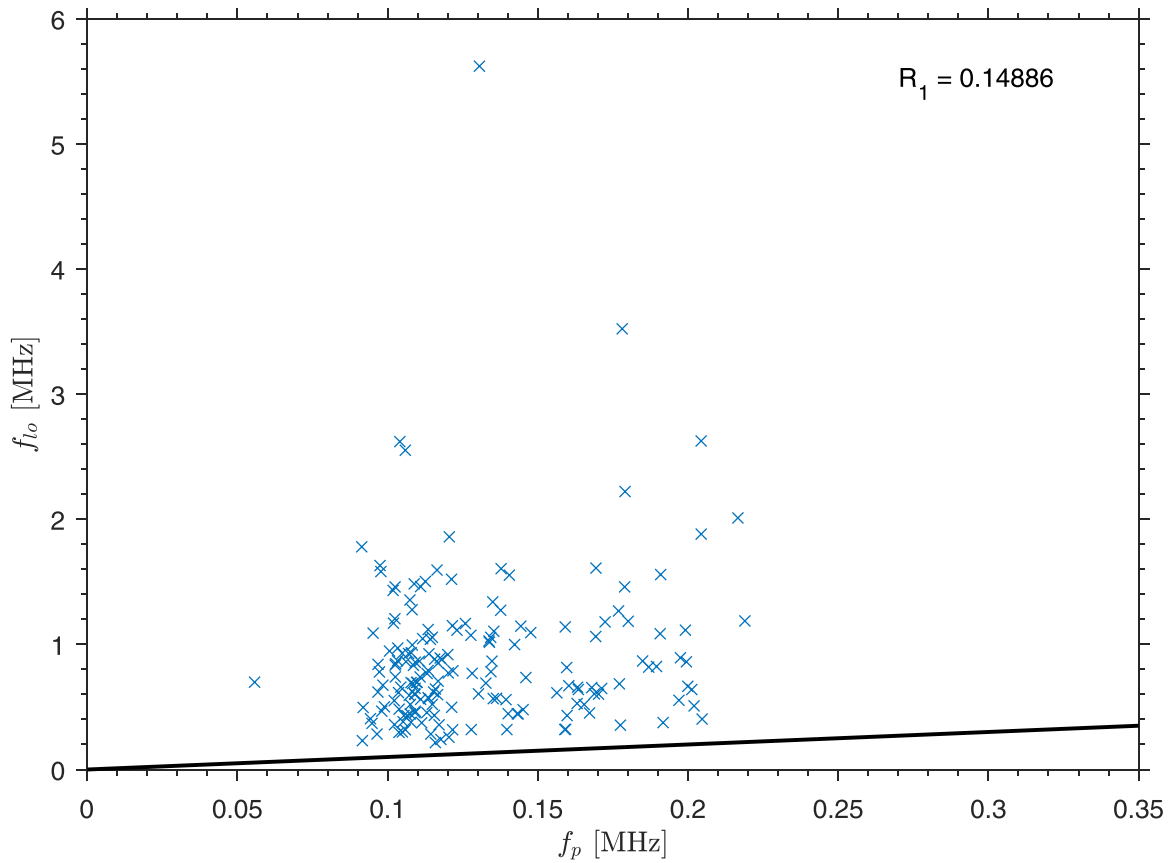
Figure 1(c), and many type III bursts with relatively weak emission intensity lower than the recognition threshold, as shown in Figure 1(d), have not been recognized by the program, and have not been included in the selected 176 events.

Figure 2 is the probability histogram of both the  $f_{lo}$  and  $f_p$  for all the 176 selected type III events. The distribution of low frequency cutoffs  $f_{lo}$  is labeled by blue bars while the distribution of plasma frequencies  $f_p$  is marked by orange bars. Here, a few events with the higher cutoff frequency in the range from 2 MHz to 6 MHz are not shown. From Figure 2, we can see that the local plasma frequency  $f_p$  distributes in a narrow range from 50 to 250 kHz and concentrates mainly within a frequency band between 100 and 150 kHz with a peak frequency  $f_p = 107$  kHz. While, on the other hand, the distribution of the cutoff frequency  $f_{lo}$  covers a much wider range from 200 kHz to over 2 MHz and concentrates mainly in a band between 0.2 MHz and 1.2 MHz with a peak frequency at  $f_{lo} = 682$  kHz. It is obvious that the distribution of the burst’s cutoff frequency is higher than that of the PSP’s local plasma frequency.

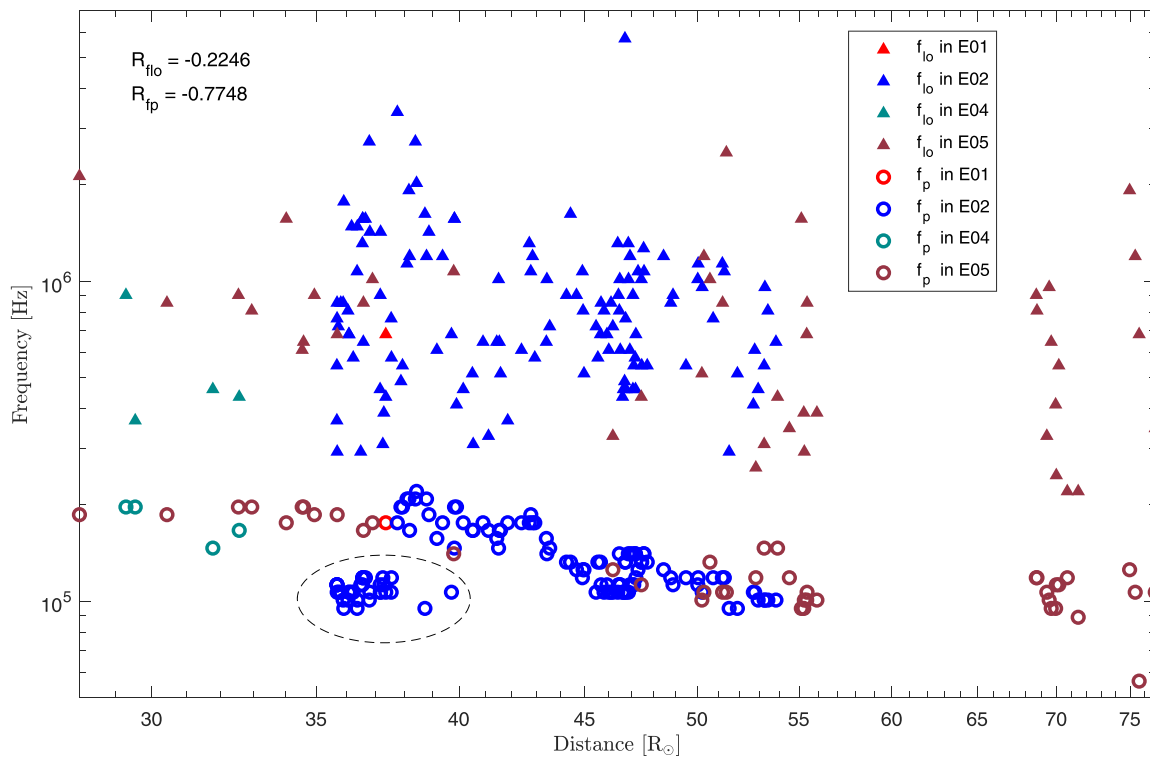
Figure 3 shows the correlation between  $f_{lo}$  and  $f_p$ . In this figure, we introduce  $\pm 5\%$  random number of  $f_{lo}$  and  $f_p$  for each point to avoid overlap among them. The blue crosses and black line represent 176 events and the position where  $f_{lo}$  equals  $f_p$ , respectively. From Figure 3, it can be found that all crosses locate clearly above the black line, which gives the same conclusion as Figure 2 that the  $f_{lo}$  spreads higher than the  $f_p$ . Their correlation coefficient  $R_1 = 0.14886$  suggests that bursts’ cutoffs are independent of the plasma frequency. In other words, the  $f_{lo}$  does not obviously depend upon the electron density around the PSP spacecraft.

Figure 4 shows the scatter plot of  $f_{lo}$  and  $f_p$  versus the distance of PSP from the Sun. The correlation coefficient  $R_{f_{lo}} = -0.2246$  implies that  $f_{lo}$  is independent of the spacecraft’s position. From Figure 4, one can find that  $f_p$  decreases with the distance if the events with relatively lower  $f_p$  in 35–40 $R_{\odot}$  circled by the black dashed line are excluded, which are associated with a high velocity solar wind stream with low density (Halekas et al. 2020). On the other hand, excluding the events circled by the black dashed line, the correlation coefficient  $R_{f_p} = -0.7748$  implies there is apparent dependency between  $f_p$  and distance of PSP from the Sun.

In the previous investigations by Leblanc et al. (1995) and Dulk et al. (1996), based on Ulysses and Wind, the observation showed that  $f_{lo}$  is almost all higher than  $f_p$ , which is also verified by the results in this study. As expected, due to the PSP being much closer to the Sun, the distribution of  $f_p$  observed by the PSP spacecraft is higher than that by Wind and Ulysses. Their results also showed that the distribution of  $f_{lo}$  is nearly unchanged with the variation of the position of spacecraft and mainly spreads in the range from 20 to 300 kHz, and the maximum probability of the cutoff frequencies is about 100 kHz (Leblanc et al. 1995; Dulk et al. 1996). Therefore, there is a significant difference between the distributions of  $f_{lo}$  in the observation by PSP in this study and in previous work based on Ulysses and Wind by Leblanc et al. (1995) and Dulk et al. (1996). Specifically, the major range of cutoff frequency is 200 kHz–1.6 MHz and the maximum probability is  $\sim 680$  kHz by PSP, which are remarkably higher than that range of 20–300 kHz and 100 kHz based on Ulysses or Wind, respectively. This considerable discrepancy between the cutoff frequencies observed by Wind and Ulysses and by PSP is a



**Figure 3.** The scatter plot of cutoff frequency  $f_{lo}$  vs. plasma frequency  $f_p$  for all the 176 events. The blue crosses represent 176 events and the black line indicates the position where the  $f_{lo}$  is equal to the  $f_p$ . Correlation coefficient  $R_1 = 0.14886$  shows there is no apparent dependency between  $f_{lo}$  and  $f_p$ .



**Figure 4.** Measurements of characteristic frequencies ( $f_{lo}$  and  $f_p$ ) of 176 type III events vs. the corresponding distances of PSP from the Sun. The solid triangle and the hollow circle indicate  $f_{lo}$  and  $f_p$ , respectively. Different colors of marks denote different encounter phases of PSP. Some events with relatively lower  $f_p$  in 35–40 $R_{\odot}$  during E02 are circled by the black dashed line.

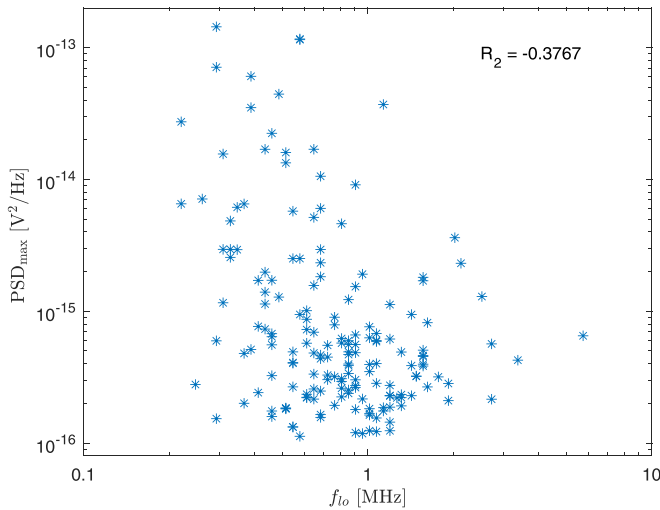


**Figure 5.** Scatter plot of the maximal power spectral density ( $\text{PSD}_{\text{max}}$ ) vs. the cutoff frequencies  $f_{lo}$  of all 176 bursts. The blue asterisks represent 176 events collected in this study.

problem worth discussing further. Below we briefly discuss some possible reasons to be responsible for this discrepancy.

First, we note that the type III events in the work of Leblanc et al. (1995) and Dulk et al. (1996) are gathered during the peak years of solar activity but this work by PSP is observed during the valley years of solar activity. It is commonly believed that type III solar radio bursts are produced directly by flare-associated energetic electron beams traveling along solar magnetic fields. In general, these energetic electron beams during the peak years of solar activity have greater energies and higher intensities and hence travel for further distances than those during the valley years of solar activity. Some studies proposed that there are many small and weak energetic electron beams that presented in the inner heliosphere but have not been detected at 1 au (Wibberenz & Cane 2006; Wang et al. 2012). Based on the observations of PSP, Mitchell et al. (2020) further confirmed the existence of these small electron events, which are associated with type III radio bursts. Therefore, the stronger electron beams during the peak years can travel further distances from the Sun and hence lead to the corresponding type III radio bursts extending to lower cutoff frequencies. While during the valley years the weaker electron beams may merge into the ambient plasma at smaller distance from the Sun and result in their type III radio bursts ending at higher cutoff frequencies.

Second, the method of selecting type III burst events also has an important influence on the analysis results. Figure 5 displays a scatter plot of the maximal power spectral density ( $\text{PSD}_{\text{max}}$ ) versus the cutoff frequencies ( $f_{lo}$ ) of all 176 bursts denoted by the blue asterisks. From Figure 5, it can be found that the  $\text{PSD}_{\text{max}}$  of type III bursts with lower  $f_{lo}$  ( $<1$  MHz) can distribute in a very wide range from low  $\sim 10^{-16}$   $\text{V}^2 \text{Hz}^{-1}$  up to over  $10^{-13}$   $\text{V}^2 \text{Hz}^{-1}$ , but the  $\text{PSD}_{\text{max}}$  with higher  $f_{lo}$  ( $>1$  MHz) is well below  $10^{-14}$   $\text{V}^2 \text{Hz}^{-1}$ . This implies that the type III bursts with higher  $f_{lo}$  usually have lower intensities. The correlation coefficient  $R_2 = -0.3767$  between  $\text{PSD}_{\text{max}}$  and  $f_{lo}$  also illustrates that they are probably related. Therefore, in vast samples by Wind and Ulysses some type III bursts with higher  $f_{lo}$  probably have been neglected because of their weakness.

Third, from Figure 1 in the previous work by Dulk et al. (1996), we can clearly see that many type III bursts with higher cutoff frequencies observed by Wind have not even been

recorded by Ulysses, located much farther from the Sun. Therefore, we speculate that the bursts with weak intensities similar to Figure 1(b) and higher cutoff frequencies can only be detected by the spacecraft located closer to the Sun.

### 3. Summary and Discussion

Type III radio bursts are the most important kind of solar radio bursts because they are closely related to fast electron beams as well as most frequently observed during solar activities. Both the plasma emission and electron cyclotron maser emission have been widely investigated and suggested as the emitting mechanism of type III radio bursts. Based on Wind and Ulysses, the work showed that cutoff frequencies  $f_{lo}$ , which are independent of the location of the spacecraft, are almost all higher than local  $f_p$  in different locations of spacecraft (Leblanc et al. 1995; Dulk et al. 1996). They proposed that low frequency cutoff is an intrinsic property of the radiation mechanism. Later, Wu et al. (2004) explained successfully the observation results by the ECME mechanism combined with the hypothesis of the density-depleted flux tubes model.

By using the RFS data gathered during the encounter phases 1–5 of PSP, we obtain 176 type III radio bursts in total, in which the  $f_{lo}$  and  $f_p$  could be precisely recognized. The statistical results show that the major frequency range of emission cutoffs spreads from 200 kHz to 1.6 MHz and the dominated distribution of  $f_{lo}$  is about 0.2–1.2 MHz with the most probable value of  $f_{lo} \sim 680$  kHz. The plasma frequency  $f_p$  spreads from 50 to 250 kHz and the dominated distribution of  $f_p$  is about 100–150 kHz with the most probable value of  $f_p \sim 100$  kHz. This means that cutoff frequencies are much higher than plasma frequency ( $f_{lo} > f_p$ ).


However, in contrast to the range of  $f_{lo}$  (20–300 kHz) observed by Wind and Ulysses, the cutoff frequencies (200 kHz–1.6 MHz) observed by PSP are much higher. In particular, the result that dominated cutoff frequencies measured by PSP (i.e.,  $\sim 680$  kHz) is significantly higher than that by Wind and Ulysses (i.e.,  $\sim 100$  kHz) needs to be explained. We propose that (1) the period of observations by Ulysses and Wind in previous work (Leblanc et al. 1995; Dulk et al. 1996) is near the solar maximum while the data analyzed in our study by PSP are gathered during the solar minimum. The solar activity intensity may affect the magnetic energy release and the propagation distance of electron beams in active regions, which can influence the growth of the radiated electromagnetic wave, and then make the distribution of cutoff frequency vary in different solar activity periods. (2) The criteria of event selection may also play an important role. We find that many weak events with higher  $f_{lo}$  could be chosen based on our selection criteria. While Leblanc et al. (1995) and Dulk et al. (1996) only considered the much stronger bursts, which are visible in 24 hr dynamic spectra. It could explain the difference of  $f_{lo}$  measured by PSP in this study from previous researchers to some extent. (3) The spacecraft located further from the Sun may be hard to receive the emission of weak bursts with higher cutoff frequencies due to the radiation attenuation effect, and thus the statistics of  $f_{lo}$  observed especially by Ulysses only covered the stronger events with lower  $f_{lo}$ . While the PSP located within 0.25 au can observe more weak bursts with higher cutoff frequencies. Excepting for these three possible reasons, we also note that PSP have shorter and thicker antennas than Wind and Ulysses. Therefore, in the PSP data, shot noise is more prominent in the low frequency below  $\sim 100$  kHz, and it will affect the recognition of the cutoff frequency of type III bursts. However, we eliminate the background involving the shot noise before we recognize the

$f_{lo}$  and hence this will significantly decrease the influence of shot noise determined by antenna geometry.

It is not yet clear which one is dominant among the three possible reasons. The statistics of multipoint observation by spacecraft like PSP, Wind, or Solar Orbiter may provide more details about the influence factors of the low frequency cutoffs of type III bursts. The work will be carried out in the near future, and we hope to give more convective explanations.

The present research at PMO was supported by NSFC under grant Nos. 41531071, BK20191513, 11873018, 11790302, and 11761131007. We hope to acknowledge the FIELDS instrument group. Their experiment on the PSP spacecraft was designed and developed under NASA contract NNN06AA01C. The FIELDS data could be obtained on the website: <https://spdf.gsfc.nasa.gov/pub/data/psp/fields/>.

#### ORCID iDs

Bing Ma  <https://orcid.org/0000-0003-0888-8879>  
 Ling Chen  <https://orcid.org/0000-0001-8058-2765>  
 Dejin Wu  <https://orcid.org/0000-0003-2418-5508>  
 Stuart D. Bale  <https://orcid.org/0000-0002-1989-3596>

#### References

- Bale, S. D., Goetz, K., Harvey, P. R., et al. 2016, *SSRv*, 204, 49  
 Chen, L., Wu, D. J., Zhao, G. Q., & Tang, J. F. 2017, *JGRA*, 122, 35  
 Dulk, G. A., Leblanc, Y., Bougeret, J.-L., & Hoang, S. 1996, *GeoRL*, 23, 1203  
 Fox, N. J., Velli, M. C., Bale, S. D., et al. 2016, *SSRv*, 204, 7  
 Ginzburg, V. L., & Zhelezniakov, V. V. 1958, *SvA*, 2, 653  
 Halekas, J. S., Whittlesey, P., Larson, D. E., et al. 2020, *ApJS*, 246, 22  
 Leblanc, Y., Dulk, G. A., & Hoang, S. 1995, *GeoRL*, 22, 3429  
 Lobzin, V. V., Cairns, I. H., & Zaslavsky, A. 2014, *JGRA*, 119, 742  
 Meyer-Vernet, N. 1979, *JGRA*, 84, 5373  
 Mitchell, J. G., de Nolfo, G. A., Hill, M. E., et al. 2020, *ApJ*, 902, 20  
 Pulupa, M., Bale, S. D., Badman, S. T., et al. 2020, *ApJS*, 246, 49  
 Pulupa, M., Bale, S. D., Bonnell, J. W., et al. 2017, *JGRA*, 122, 2836  
 Schneider, J. 1959, *PhRvL*, 2, 504  
 Twiss, R. Q. 1958, *AuJPh*, 11, 564  
 Wang, L., Lin, R. P., Krucker, S., & Mason, G. M. 2012, *ApJ*, 759, 69  
 Wibberenz, G., & Cane, H. V. 2006, *ApJ*, 650, 1199  
 Wild, J. P., & McCready, L. L. 1950, *AuSRA*, 3, 387  
 Wild, J. P., Murray, J. D., & Rowe, W. C. 1954a, *AuJPh*, 7, 439  
 Wild, J. P., Roberts, J. A., & Murray, J. D. 1954b, *Natur*, 173, 532  
 Wu, C. 2012, *ChSBu*, 57, 1357  
 Wu, C. S., Reiner, M. J., Yoon, P. H., Zheng, H. N., & Wang, S. 2004, *ApJ*, 605, 503  
 Wu, C. S., Wang, C. B., Yoon, P. H., Zheng, H. N., & Wang, S. 2002, *ApJ*, 575, 1094